THE NICKEL-YTTRIUM PHASE DIAGRAM

by

Bernard Joseph Beaudry

16

A Thesis Submitted to the
Graduate Faculty in Partial Fulfillment of
The Requirements for the Degree of
MASTER OF SCIENCE

Major Subject: Metallurgy

Iowa State University
Of Science and Technology
Ames, Iowa

1959

TABLE OF CONTENTS

$1126-18$

I. INTRODUCTION

In the present day search for new metals, interest has arisen in yttrium metal due to its high melting point and moderately low density. Its low neutron capture cross-section also makes it an interesting metal for use in nuclear reactors. The results of Haefling's (1) investigation of the immiscibility of uranium with the rare earth metals and yttrium suggested the use of yttrium as a container for uranium and uranium base alloys. Subsequently, Fisher and Fullhart (2) found an yttrium crucible would contain molten uranium-chromium eutectic for 3000 hours without appreciable attack. To protect the yttrium from atmospheric corrosion in this work, it was clad with a nickel-rich stainless steel; however, a low melting phase formed where the yttrium was in contact with the steel. To investigate the cause of this phenomenon, Haefling (3) made a survey study of yttrium systems with chromium, manganese, iron and nickel and found an 18 wt. % Ni (weight percent) alloy to melt at approximately 900°C. No other reference to work on nickel-yttrium alloys was found in the literature.

An application of Hume-Rothery's rules of alloying based on size factor, electronegativity and valency predicted negligible terminal solubility and possible compound formation due to the electronegativity differences of

yttrium and nickel.

Vogel (4) in a study of the systems of cerium, lanthanum and praseodymium with nickel found 6 compounds of the same formula in each system, i.e., R_3Ni, RNi, RNi_2, RNi_3, RNi_4, and RNi_5. Since there is a great similarity between yttrium and the rare earths, compound formation was likely to occur also in the yttrium-nickel system. Vogel (4) observed that the ability to form compounds with the rare earths diminishes in the order nickel, cobalt and iron while no compounds are formed with manganese, chromium and titanium. Available data on yttrium systems with these elements indicate similar behavior, except that a slightly greater tendency toward compound formation occurs. Simple eutectics with limited solid solubility have been found in the yttrium-titanium (5) and yttrium-chromium (3) systems, but at least 1 compound, YMn_2 (3) is present in the yttrium-manganese system. In the case of yttrium-iron, at least 4 compounds are present (3), while only 2 are present in the cerium-iron (6) and no compounds are present in the lanthanum-iron (3) system. Metallographic examination by the author of 2 alloys in the central portion of the yttrium-cobalt system showed at least 3 intermetallic compounds present in this system.

The alloying behavior of plutonium might also be used in predicting the nature of the yttrium-nickel system. As

is the case with the rare earth-nickel systems 6 compounds are also present in the plutonium-nickel system (7); PuNi, $PuNi_2$, $PuNi_3$, $PuNi_4$, $PuNi_5$ and Pu_2Ni_{17}. The latter compound is not present in the cerium-nickel system and the Ce_3Ni prototype is not present in the plutonium-nickel system.

In discussing the alloying behavior of plutonium, Konobeevsky (8) noted that there is an increase in the number of intermetallic compounds formed with plutonium with increasing atomic number of the transition element - an observation very similar to that of Vogel's (4) concerning the rare earth metals and the first transition series. Ellinger (9), in a review of the intermetallic compounds of plutonium, points out that the transition metals of group VIII and the B subgroup elements tend to form the most intermetallic compounds with plutonium.

On the basis of the trend in the alloying behavior of yttrium with the first transition series as compared with the trend noted by Vogel (4) for the alloying behavior of the rare earths with these elements, the large number of compounds in the Ce-Ni system, and the alloying behavior of plutonium with nickel, one might expect at least 6 compounds to form in the nickel-yttrium system. The present study was undertaken to confirm these predictions of low terminal solid solubility and compound formation and to establish the general alloying behavior of yttrium with nickel.

II. EXPERIMENTAL

A. Materials

The nickel employed in this investigation was "Baker Analyzed" reagent nickel shot of 99.9% purity. The major impurities in the nickel were: 30 ppm Pb, 80 ppm Co and 400 ppm Fe. Trace amounts of Cr, Cu, Mg, Si and Ca were also present. The impurities in the yttrium used can be divided into 2 types - metallic and non-metallic. The major metallic impurities were 180 ppm Si, 100 ppm Fe, 50 ppm Cu, 30 ppm Mg, 10 ppm Ca and 5000 ppm Ta or a total metallic impurity of approximately 0.54 wt. %. Tantalum was introduced into the yttrium metal during the reduction process in tantalum crucibles. The major non-metallic impurities were 1700 ppm O_2, 200 ppm C, and 430 ppm N_2 or a total non-metallic impurity of approximately 0.23 wt. %.

To calculate the amount of yttrium metal present in the samples, it was assumed that the oxygen, nitrogen, and carbon were present as Y_2O_3, YN, and Y_3C. It is believed that these compounds present in the yttrium did not enter the alloying reaction since the heats of formation of yttrium carbide, nitride and oxide are considerably higher than the nickel carbide, nitride and oxide. In addition, dendrites of these impurities were still present in the alloys.

B. Preparation of Alloys

All the alloys examined were initially formed by co-melting the 2 metals in an arc melting furnace. The buttons were inverted at least 3 times and remelted each time to ensure homogeneity. Negligible weight loss occurred during the arc melting process, maintaining the intended composition of the alloy during preparation. Chemical analysis of the alloys in all cases was within 0.5 at. % (atomic percent) of the intended composition.

C. Examination of Alloys

1. Thermal methods

The principle method used was time-temperature thermal analysis employing Chromel-Alumel thermocouples in the low melting portion of the diagram from 25 to 66 at. % nickel, and Pt—Pt-13%Rh thermocouples in the remaining portions. The furnace used for thermal analysis was a split-tube graphite resistance furnace shown schematically in Fig. 1. This furnace was operated in either a vacuum or an inert gas atmosphere and could easily reach $1600^{\circ}C$ under these conditions. A 10 KVA stepdown transformer supplied approximately 2¼ KVA of power at 10 volts to achieve the highest temperature.

Several different crucibles were used depending on the composition of the alloys. Tantalum crucibles worked well
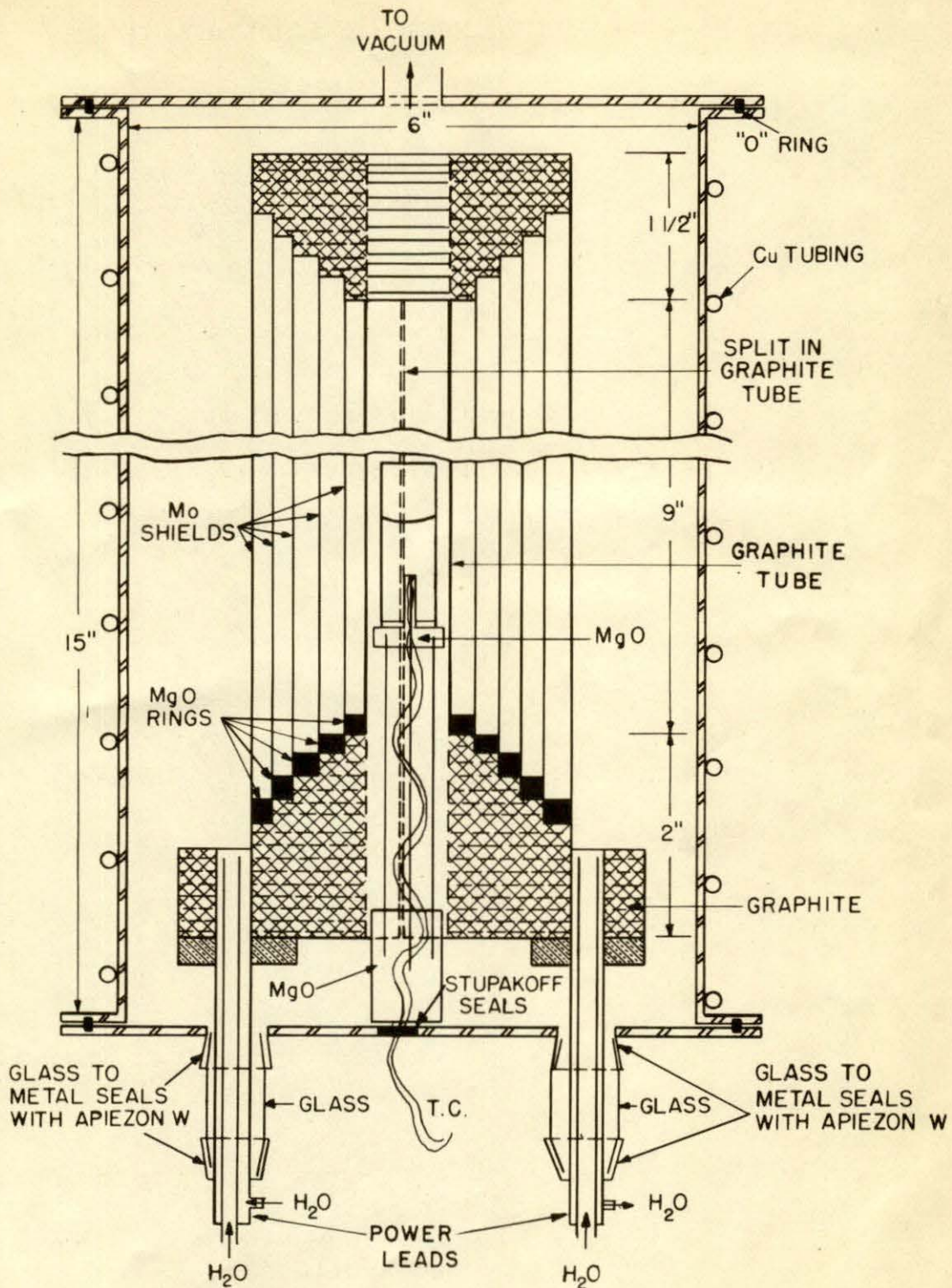
Fig. 1. Schematic diagram of the furnace used for thermal analysis.

from 0 to 50 at. % Ni, but a reaction between the crucible
and melt was noted with greater than 50 at. % Ni. MgO cru-
cibles were used from 50 to 66 at. % Ni, but when the maxi-
mum temperature required in thermal analysis exceeded
$1150^{\circ}C$, a reaction occurred between the crucible and melt
depositing a white powder between the melt and crucible.
X-ray analysis of this white powder showed it to be Y_2O_3
resulting from the reaction of yttrium with MgO. Since the
Y_2O_3 did not dissolve in the alloy, the use of Y_2O_3 as a
suitable crucible material was indicated. The ceramic fab-
rication department of the Ames Laboratory fabricated Y_2O_3
crucibles which proved to be very satisfactory for thermal
analyses of alloys from 67 to 100 at. % Ni.

The "bottom" thermocouple arrangement shown in Fig. 1
was used only when tantalum crucibles were used, due to the
difficulty of fabricating bottom thermocouple wells in ce-
ramic crucibles. When the thermocouple was placed in the
furnace from the top, "vitreous refractory mullite" tubes
obtained from the McDanel Refractory Procelain Company con-
taining 53 wt. % Al_2O_3 and 47 wt. % SiO_2 were used as ther-
mocouple wells. The inside dimensions of all crucibles used
were 3/4" X 2½" high. After initial formation in the arc-
melting furnace, the alloys containing from 25 to 95 at. %
Ni were brittle, enabling them to be crushed in a diamond
mortar and placed in the crucible. Alloys containing 0 to

25 and 95 to 100 at. % Ni were less brittle and were cast
into the crucibles by induction heating before thermal anal-
ysis. The thermocouple was positioned so as to be 1/3 the
height of the melt from the bottom of the crucible.

A constant heating and cooling rate of 5 degrees per
minute was obtained by a motor drive on a variable trans-
former connected in series with the step-down transformer.
As will be discussed later, faster heating and cooling rates
obtained by manual operation of the variable transformer
were used in the region from 70 to 83 at. % Ni to establish
the peritectic horizontals in this region. The heating and
cooling curves were plotted automatically on a 2-pen Bristol
recording potentiometer.

The Pirani and Alterthum (10) method, commonly known as
the melting point bar method, was used on 3 alloys between
91 and 97 at. % Ni to establish the melting point of the
Y_2Ni_{17}-Ni eutectic. The results were later verified by
thermal analysis.

Annealing and quenching studies were made of various
alloys to establish the composition of peritectic compounds,
the composition range, if any, of the various compounds in
the system, and the solubility limits of the metals in each
other. To anneal below $800^{\circ}C$, the samples were sealed in
Vycor under a partial atmosphere of helium, while samples to
be annealed between 800 and $1100^{\circ}C$ were sealed in silica.

To anneal at temperatures between 1100 and 1250°C, the samples were sealed in type 304 stainless steel bombs with yttria liners under a partial atmosphere of helium. Quenching of the samples was carried out by dropping the capsules into water and breaking the capsule immediately after contacting water. Since the stainless steel bombs did not permit fracture, quenching rates were naturally slower. However, from a temperature of 1250°C, the bombs were below a red heat in 5 seconds and at room temperature in 15 seconds.

2. Metallographic methods

Standard polishing techniques were used in the preparation of samples for metallographic examination. An etchant containing $3/4\%$ HNO_3 by volume in absolute alcohol ($3/4\%$ nital) was found to be satisfactory for alloys from 0 to 60 at. $\%$ Ni with etching times ranging from 1 to 15 seconds, while a 5% solution of HNO_3 by volume in absolute alcohol (5% nital) was used for alloys from 60 to 84 at. $\%$ Ni. For alloys containing from 84 to 99 at. $\%$ Ni, a solution containing 1 part concentrated nitric acid, 1 part concentrated acetic acid and 1 part water was used and Carapella's reagent which contains 5 g. of ferric chloride, 2 ml. of concentrated hydrochloric acid and 99 ml. of absolute alcohol was used for alloys between 99 and 100 at. $\%$ Ni.

3. X-ray methods

Single crystal methods were used to characterize the 3 intermetallic compounds YNi, YNi_3 and Y_2Ni_{17}. The single crystals were obtained from shrinkage cavities of alloys containing 53, 70 and 91.5 at. % Ni in which the phases studied were the primary phase. The lattice constants of these compounds were determined from rotation patterns and zero level Weissenberg photographs.

Powder patterns taken with a 57.3 mm. radius Debye-Scherer camera using CuK_α radiation were used to identify the various phases present in multi-phased alloys; to determine the lattice constants of YNi_2 and YNi_5; and to verify the structure of YNi_2 and YNi_5. Powder specimens of the massive samples were prepared by filing or crushing the alloy, placing the powder in pyrex capillaries and annealing for 3 hours at $400^{\circ}C$ to remove the effects of cold working. To identify the phases in multi-phased alloys, the alloys were first polished and etched, then samples for X-ray analysis of each phase were cut out under a binocular microscope using a biological scalpel.

The lattice constants of YNi_2 and YNi_5 were determined by a Cohen's (11) least squares treatment on an IBM 650 computer. In order to establish the composition range of YNi_2, alloys from each side of YNi_2 were annealed at $950^{\circ}C$, quenched and the lattice constant of YNi_2 in each alloy was

determined. Since the unit cell was smaller on the nickel-rich side of YNi_2, the composition range of the YNi_2 was calculated by assuming the volume contraction was due to the substitution of nickel for yttrium in the lattice.

4. Density determination method

The density of each phase for which lattice constants were obtained was determined by conventional pycnometric methods using CCl_4 as the immersion fluid. A 10.629 cc. pycnometer and 4 cc. of sample were used.

5. Magnetic transition temperature determination method

The magnetic transition temperature of nickel and nickel-rich alloys was determined by observing the temperature at which the magnetic force of attraction between the sample and an Alnico magnet changed suddenly on heating and cooling. Though the method was rather crude, good precision was obtained. The temperatures noted on heating were $356^{\circ}C$ (Pure Ni), $358^{\circ}C$ (96.3 at. % Ni), and $356^{\circ}C$ (93.2 at. % Ni) while the temperature noted on cooling was $350^{\circ}C$ in all 3 cases.

III. PRESENTATION AND INTERPRETATION OF RESULTS

The phase diagram shown in Fig. 2 was constructed from results of thermal, metallographic and X-ray studies on the Ni-Y system.

The formulas assigned YNi_2 and YNi_5 by thermal and metallographic studies were confirmed by a structure analysis, while the formulas assigned YNi, YNi_3 and Y_2Ni_{17} were verified by measured density and unit cell volume considerations. The formulas Y_3Ni, Y_3Ni_2, Y_2Ni_7 and YNi_4 were assigned from thermal and metallographic studies, and their existence was verified by X-ray studies. Evidence for the composition range indicated for YNi_2 and YNi_5 by dashed lines in Fig. 2 was observed experimentally as will be discussed later, but since a complete study of composition versus temperature was not made, only an estimate of the slope of the solvus is presented.

A. Thermal Results

The results of thermal analysis are plotted graphically in Fig. 2. A tabulation is made in Table 1 of the composition and melting point of the intermetallic compounds and the eutectics, and the melting point of the pure metals.

Changes in slope for the liquidus on time-temperature curves were easily observed with heating and cooling rates of 5 degrees per minute over the entire composition range.
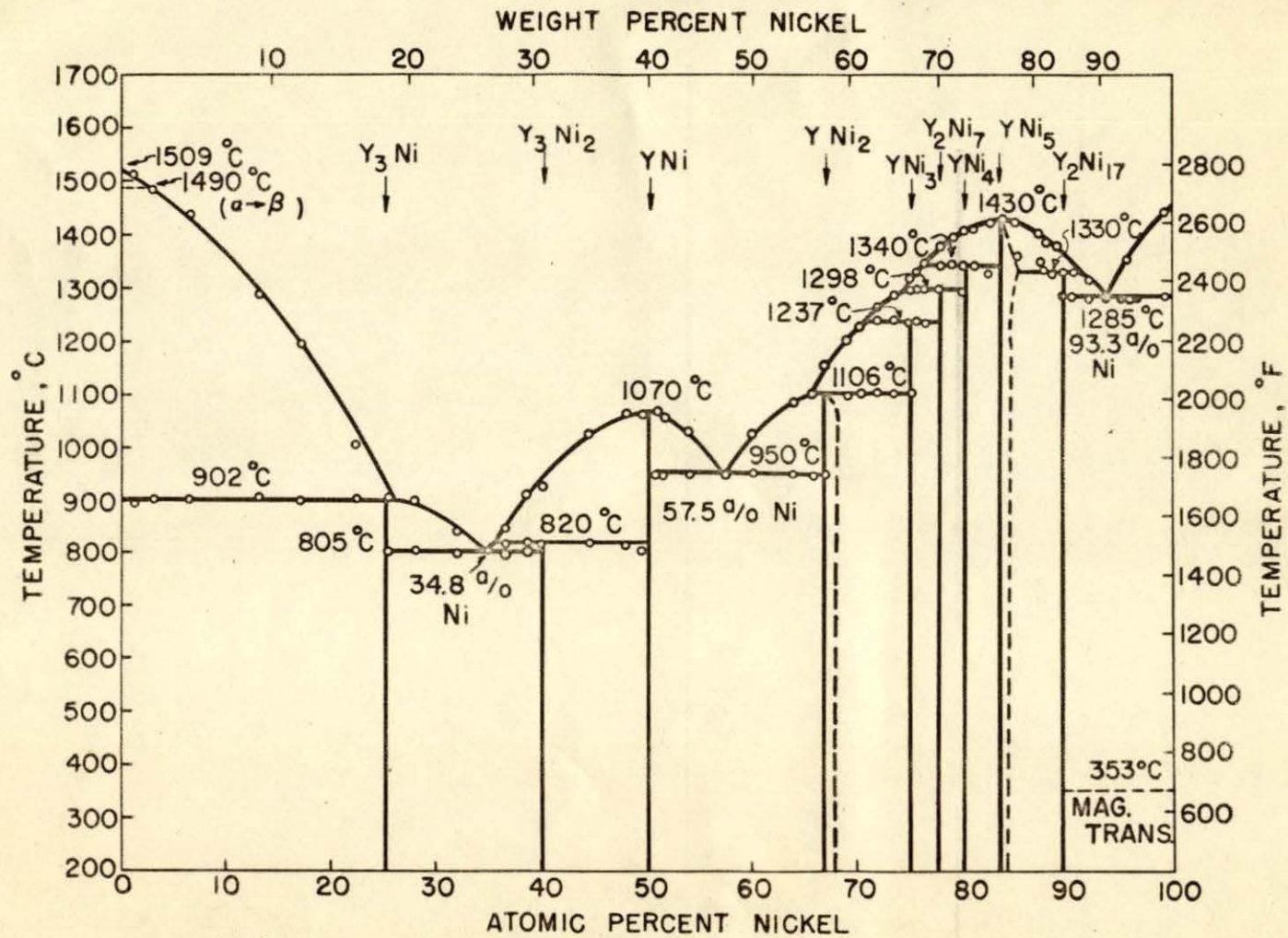
Fig. 2.   The nickel-yttrium phase diagram.

Table 1. Melting points of metals and alloys.

Formula	Nominal composition		Type of melting	Temperature of melting	
	at.%Ni	wt.%Ni		°C	°F
Y			Congruent	1509±5	2768±18
Y_3Ni	25.00	18.03	Incongruent	902±4	1656±7
Y_3Ni_2	40.00	30.56	Incongruent	820±4	1508±7
YNi	50.00	39.76	Congruent	1070±3	1958±5
YNi_2	66.67	56.90	Incongruent	1106±3	2023±5
YNi_3	75.00	66.44	Incongruent	1237±5	2259±9
Y_2Ni_7	77.78	69.79	Incongruent	1298±5	2368±9
YNi_4	80.00	72.53	Incongruent	1340±8	2444±14
YNi_5	83.33	76.75	Congruent	1430±5	2606±9
Y_2Ni_{17}	89.47	84.87	Incongruent	1330±10	2426±18
Ni	100	100	Congruent	1455±3	2651±5
Eutectic					
$Y_3Ni-Y_3Ni_2$	34.80	26.05	----------	805±4	1481±7
$YNi-YNi_2$	57.50	47.18	----------	950±3	1742±5
$Y_2Ni_{17}-Ni$	93.30	90.18	----------	1285±5	2345±9

Isothermal arrests were observed for the various solidus temperatures from 0 to 70 at. % Ni and from 83 to 100 at. % Ni with the same heating and cooling rate. However, in the region from 70 to 83 at. % Ni, due to the large number of overlapping peritectic horizontals, only slight changes in slope were observed for the various horizontals when rates of 5 degrees per minute were used. It was found that rates of approximately 40 degrees per minute gave short, reproducible isothermal arrests for each horizontal. The reproducibility of these arrests on heating and cooling ($\pm$ 5°C) was taken as evidence for the accuracy of this method.

Due to the large number of compounds from 66 to 84 at. % Ni, alloys were prepared at approximately 1 atomic percent intervals in this region. The points at which the peritectic horizontals of YNi_2, YNi_3, Y_2Ni_7, and YNi_4 intersect the liquidus were established by extrapolating the solidus to the liquidus. Since thermal analyses were run on alloys at small composition intervals, the amount of extrapolation necessary was small. The data for the peritectic decomposition temperature of Y_2Ni_{17} (86-91.0 at. % Ni) were not as reproducible as data for the other parts of the system, but this is believed to be due to the large curvature in the solidus of YNi_5 between 83.4 and approximately 85.0 at. % Ni. Points on the YNi_5 solidus as shown in Fig. 2 were noted as changes in slope on the time-temperature curves.

The agreement between the points obtained by thermal analysis and the method of Pirani and Alterthum (10)(shown as filled circles in Fig. 2) for the Y_2Ni_{17} - Ni eutectic horizontal was very good. Extrapolation of the thermal data indicated the Y_2Ni_{17} peritectic horizontal extends to 91.0 at. % Ni which was confirmed by metallographic methods.

B. Metallographic Results

The solubility of nickel in yttrium at 900°C was found to be approximately 0.2 at. % Ni by the disappearing phase method. A 13 at. % Ni alloy (see Fig. 3) shows alpha yttrium surrounded by the incongruent melting compound Y_3Ni. Since this alloy is in the as arc-cast condition and no eutectic is visible within the Y_3Ni grains, the peritectic horizontal of Y_3Ni apparently does not extend appreciably beyond the compound composition. This is also indicated by Fig. 4 in which a 25.4 at. % Ni alloy in the as arc-cast condition shows Y_3Ni as the primary phase. Extrapolation of thermal analysis data indicated the Y_3Ni peritectic horizontal extends to 25.6 at. % Ni as shown in Fig. 2. The formula Y_3Ni for this compound was indicated by thermal data and verified by Fig. 4 which shows a 25.4 at. % Ni alloy to be nearly 1 phase with a slight amount of eutectic surrounding the primary crystals. The composition of the Y_3Ni - Y_3Ni_2 eutectic was shown to be 34.8 at. % Ni from an alloy of this

composition which was pure eutectic (see Fig. 5).

The peritectic nature of Y_3Ni_2 is shown in Fig. 6 which is a photomicrograph of a 39.9 at. % Ni alloy in the as arc-cast condition. Primary YNi is surrounded by Y_3Ni_2 which in turn is surrounded by the Y_3Ni - Y_3Ni_2 eutectic. The formula Y_3Ni_2 was assigned this compound since the 39.9 at. % Ni alloy shown in Fig. 6 was nearly 1 phase after a homogenizing anneal at $795^{\circ}C$ for 120 hours (see Fig. 7). A 36.3 at. % Ni alloy in the as arc-cast condition still contained YNi as the primary phase (see Fig. 8) thus the Y_3Ni_2 peritectic horizontal extends to at least this composition. Extrapolation of thermal data indicated the horizontal extends to 35.7 at. % Ni.

The formula YNi was indicated by metallographic examination of a 49.8 at. % Ni alloy which contained primary YNi with a slight amount of Y_3Ni_2 in the grain boundaries (see Fig. 9). This formula was confirmed by X-ray analysis as will be discussed later.

The composition 57.5 at. % Ni was indicated for the YNi - YNi_2 eutectic since an alloy of this composition was pure eutectic (see Fig. 10). Fig. 11 shows YNi_2 in equilibrium with eutectic in a 60 at. % Ni alloy. The YNi_2 peritectic horizontal apparently does not extend beyond 65.5 at. % Ni, since an alloy of this composition in the as arc-cast condition shows YNi_2 as the primary phase (see Fig. 12).

Fig. 3. 13 at. % Ni. As arc-cast. Alpha yttrium
in a matrix of Y_3Ni. Black spots are im-
purity dendrites? Etched 1 second in
3/4% nital. X200.

Fig. 4. 25.4 at. % Ni. As arc-cast. Primary
Y_3Ni surrounded by a small amount of
eutectic. Black spots are impurity den-
drites. Etched 1 second in 3/4% nital.
X200.

Fig. 5. 34.8 at. % Ni. As arc-cast. Pure Y_3Ni -
Y_3Ni_2 eutectic. Etched 2 seconds in 3/4%
nital. X1000.

Fig. 6. 39.9 at. % Ni. As arc-cast. YNi sur-
rounded by Y_3Ni_2 in turn surrounded by
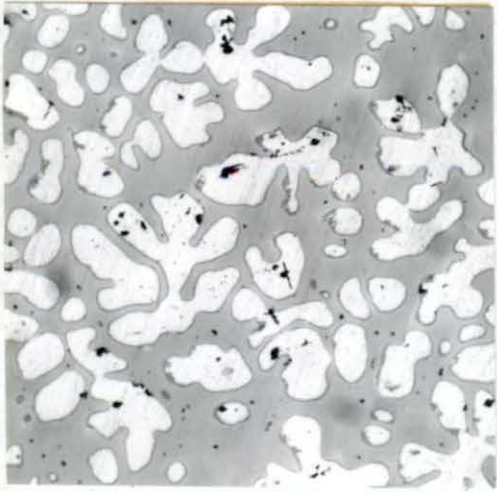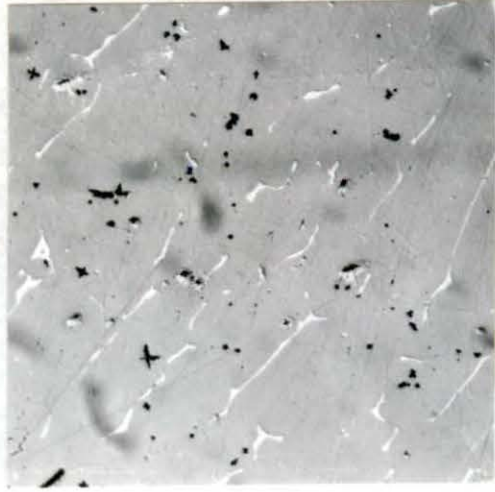eutectic. Etched 5 seconds in 3/4% nital.
X200.

Fig. 3.

Fig. 4.
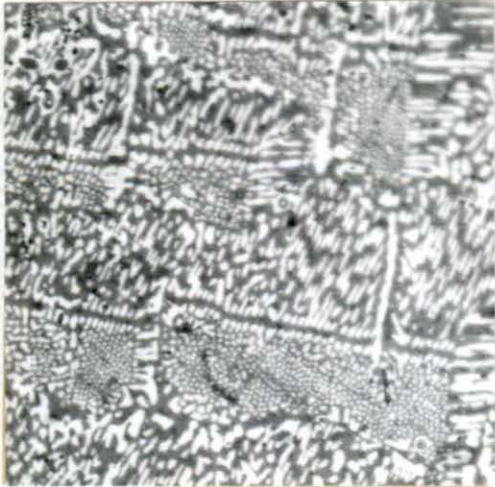
Fig. 5.
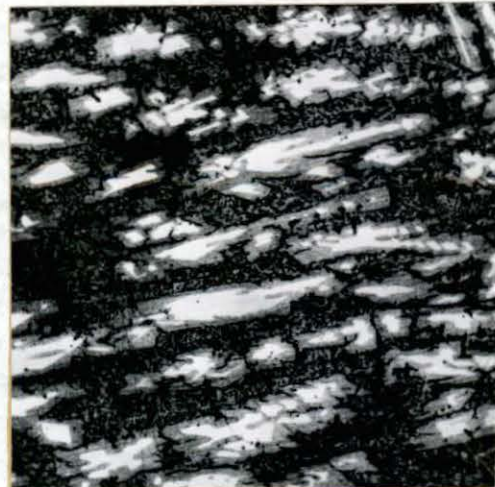
Fig. 6.

Fig. 7. 39.9 at. % Ni. Annealed at 795°C for 120 hours. Y_3Ni_2 with a slight amount of YNi. Etched 5 seconds in 3/4% nital. X200.

Fig. 8. 36.3 at. % Ni. As arc-cast. Slight amount of YNi surrounded by Y_3Ni_2 in turn surrounded by eutectic. Etched 5 seconds in 3/4% nital. X200.

Fig. 9. 49.8 at. % Ni. As arc-cast. YNi with slight amount of Y_3Ni_2 in the grain boundaries. Black spots are impurity dendrites. Etched 6 seconds in 3/4% nital. X200.

Fig. 10. 57.5 at. % Ni. As arc-cast. Pure YNi - YNi_2 eutectic. Etched 1 second in 5% nital. X1000.

Fig. 7.

Fig. 8.

Fig. 9.

Fig. 10.

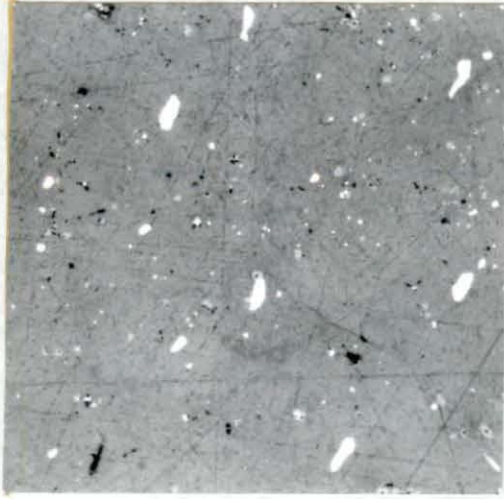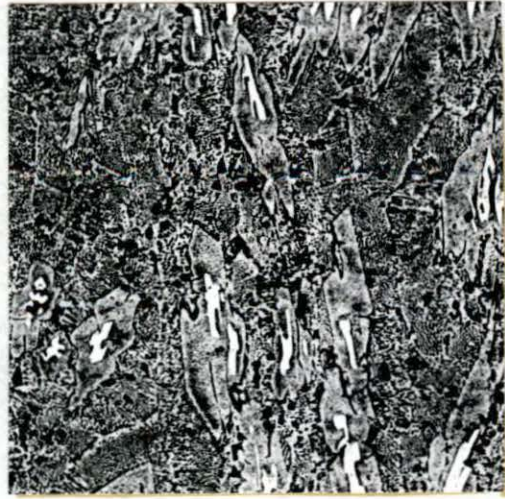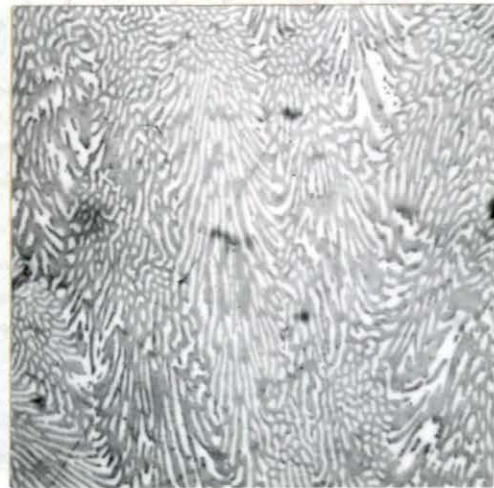The peritectic nature of the compounds YNi_2, YNi_3, Y_2Ni_7, and YNi_4 was indicated by the series of arrests obtained by thermal analysis of alloys between 66 and 83 at. % Ni. Metallographic examination of alloys in this region in the as arc-cast condition showed them to be multiphased alloys (see Fig. 13). However, when alloys of the composition of the compounds were annealed at temperatures just below their peritectic decomposition temperatures, 1 phased alloys resulted. X-ray powder patterns of these 1 phased alloys were used in the identification of the phases present in multiphased alloys.

Fig. 14 shows 1 phase present in a 66.7 at. % Ni alloy after a homogenizing anneal at $945^{\circ}C$ for 100 hours indicating the formula YNi_2. An X-ray structure analysis of this phase confirmed the formula YNi_2. The multiphased alloy (75 at. % Ni) shown in Fig. 13 was nearly 1 phase as shown in Fig. 15 after homogenizing at $1100^{\circ}C$ for 150 hours indicating the formula YNi_3. The formula YNi_3 for this compound was confirmed by X-ray diffraction studies as will be discussed later. A 77.6 at. % Ni alloy after annealing at $1150^{\circ}C$ for 240 hours was nearly 1 phase (see Fig. 16) indicating the formula Y_2Ni_7.

The phase YNi_4 is characterized metallographically by the presence of microcracks in its microstructure (see Fig. 17). Also, the lines on X-ray powder patterns of YNi_4

Fig. 11.   60.0 at. % Ni. Cooled slowly. YNi_2
plus eutectic. Etched 1 second in
5% nital. X200.

Fig. 12.   65.5 at. % Ni. As arc-cast. YNi_2
plus eutectic. Etched 1 second in
5% nital. X200.

Fig. 13.   75.0 at. % Ni. As arc-cast. Very
slight amount of YNi_4 surrounded by
Y_2Ni_7 surrounded by YNi_3 in turn sur-
rounded by YNi_2 (darkest phase).
Etched 5 seconds in 5% nital. X200.

Fig. 14.   66.7 at. % Ni. Annealed at 945°C for
100 hours and quenched. YNi_2. Etched
5 seconds in 5% nital. X200.

Fig. 11.

Fig. 12.
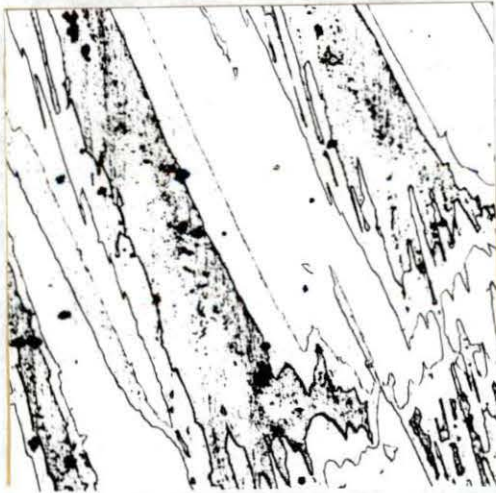
Fig. 13.
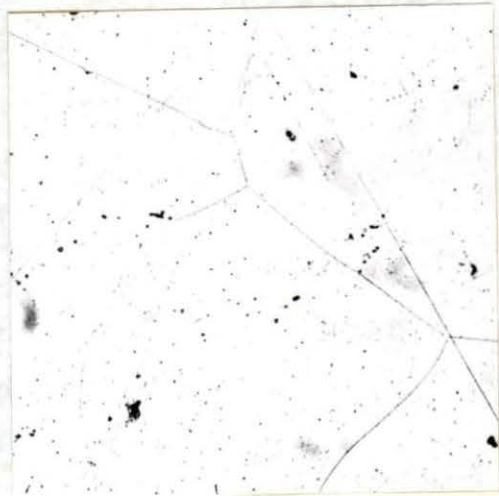
Fig. 14.

are quite diffuse in the front reflection region and fade
out completely in the back reflection region. These char-
acteristics suggested a phase transformation in this com-
pound; however, thermal analysis of an alloy containing
80.1 at. % Ni which was first homogenized at 1250°C showed
no thermal arrests between room temperature and 1330°C. The
microcracks could also be explained by a large contraction
of the unit cell in 1 direction on cooling; the resulting
distortion of the lattice would also explain the diffuse
X-ray diffraction pattern. Figs. 18 and 19 show 2-phased
alloys from each side of YNi_4 with nominal composition of
78.9 and 81.2 at. % Ni respectively. The 2 phases present
in each alloy were identified by X-ray analysis. The sam-
ples for X-ray analysis were dug out under a binocular
microscope by use of a biological scalpel.

The compound YNi_5 is shown in Fig. 20 (83.4 at. % Ni)
to be 1 phase in the as arc-cast condition indicating the
congruent nature of this compound. Thermal results also
show YNi_5 to melt congruently.

The solubility of Ni in YNi_5 was proposed from thermal,
metallographic and X-ray evidence. Points on the solidus
were obtained by thermal analysis. An 84.5 at. % Ni alloy
which had been annealed at 1150°C for 240 hours and quenched
was 1 phased (see Fig. 21). The X-ray evidence for this
composition range will be discussed later.

Fig. 15.   75.0 at. % Ni. Annealed at 1100°C
           for 150 hours and cooled rapidly.
           YNi$_3$ with slight amount of YNi$_2$
           present. Etched 15 seconds in 5%
           nital. X200.

Fig. 16.   77.6 at. % Ni. Annealed at 1150°C
           for 240 hours. Y$_2$Ni$_7$ with small
           amount of YNi$_3$ present. Etched 20
           seconds in 5% nital. X200.

Fig. 17.   80.1 at. % Ni. Annealed at 1250°C
           for 1 hour. YNi$_4$ which is typified
           by microcracks (see text). Etched
           25 seconds in 5% nital. X200.

Fig. 18.   78.9 at. % Ni. Annealed at 1150°C
           for 240 hours. YNi$_4$ (cracked phase)
           plus Y$_2$Ni$_7$. Etched 25 seconds in
           5% nital. X200.

Fig. 17.

Fig. 18.
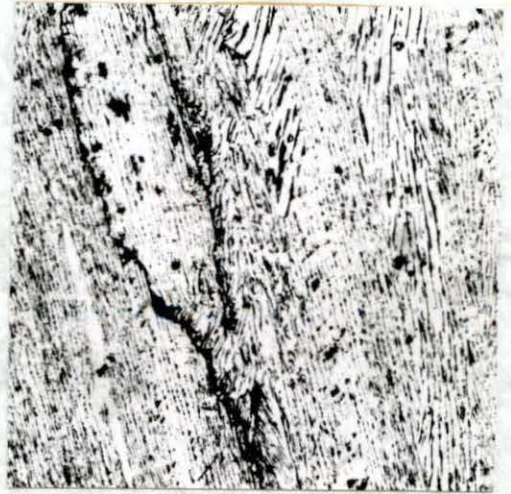
Fig. 15.

Fig. 16.

The peritectic nature of Y_2Ni_{17} was shown by peritectic rimming in an as arc-cast 89.9 at. % Ni alloy (see Fig. 22). This alloy when annealed at $1250^{\circ}C$ for 1 hour was almost pure compound with some nickel present (see Fig. 23) indicating the formula Y_2Ni_{17}. An 89.4 at. % Ni alloy was 1 phase as shown in Fig. 24 confirming the formula Y_2Ni_{17}. The Y_2Ni_{17} peritectic horizontal apparently does not extend appreciably beyond 91.0 at. % Ni, since in a 91.3 at. % Ni alloy in the as arc-cast condition, Y_2Ni_{17} is the primary phase with no peritectic rimming (see Fig. 25). Extrapolation of thermal data indicated the horizontal extends to 91.0 at. % Ni. Fig. 26 shows pure eutectic at a composition of 93.3 at. % Ni.

The solubility of yttrium in nickel was shown to be low, since a 0.33 at. % Y alloy annealed at $1250^{\circ}C$ and quenched had an appreciable amount of a second phase present (see Fig. 27) while in a 0.14 at. % Y alloy annealed at $1250^{\circ}C$ and quenched, only a slight amount of the second phase is still present (see Fig. 28).

C. X-ray Results

The results of X-ray analysis of the intermetallic compounds present in the nickel-yttrium system are outlined in Table 2. The X-ray results for each compound are discussed in the following paragraphs.

Fig. 19. 81.2 at. % Ni. Annealed at 1150°C
for 240 hours. YNi_5 plus YNi_4
(cracked phase). Etched 25 seconds
in 5% nital. X200.

Fig. 20. 83.4 at. % Ni. As arc-cast. YNi_5
with a few impurity dendrites. Etched
1 minute in 5% nital. X200.

Fig. 21. 84.5 at. % Ni. Annealed at 1150°C for
240 hours and cooled rapidly. One
phased YNi_5. Etched 1 minute in 5%
nital. X200.

Fig. 22. 89.9 at. % Ni. As arc-cast. YNi_5
surrounded by Y_2Ni_{17} surrounded by
eutectic (black due to over etching).
Etched 6 seconds in nitric-acetic-
water etchant. X200.

Fig. 20.

Fig. 22.

Fig. 19.

Fig. 21.

30
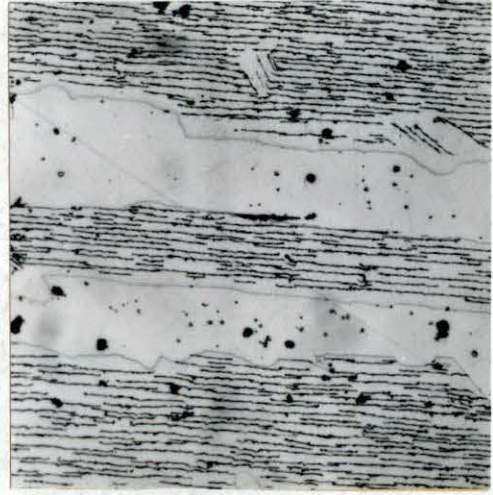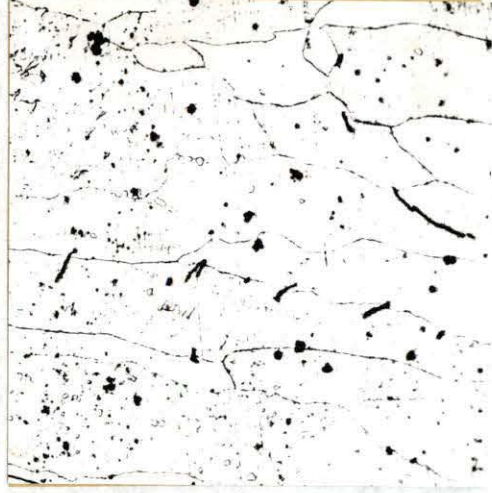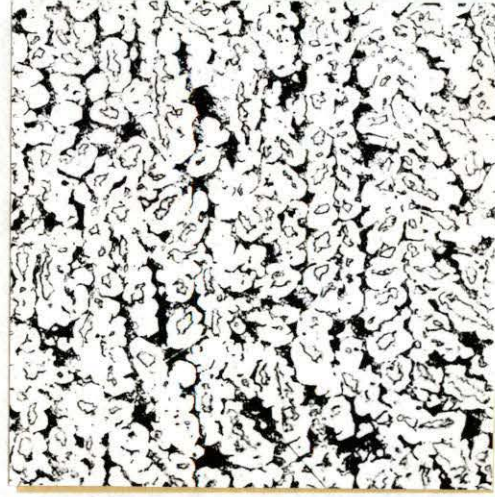
Fig. 23. 89.9 at. % Ni. Annealed at 1250°C
for 1 hour. Y_2Ni_{17} plus small amount
of nickel. Etched 4 seconds in nitric-
acetic-water etchant. X200.

Fig. 24. 89.4 at. % Ni. Annealed at 1250°C for
1 hour. Pure Y_2Ni_{17}. Etched 7 seconds
in nitric-acetic-water etchant. X200.

Fig. 25. 91.3 at. % Ni. As arc-cast. Y_2Ni_{17}
plus eutectic. Etched 6 seconds in
nitric-acetic-water etchant. X200.

Fig. 26. 93.3 at. % Ni. As arc-cast. Y_2Ni_{17}-Ni
eutectic. Etched 3 seconds in nitric-
acetic-water etchant. X500.

Fig. 23.
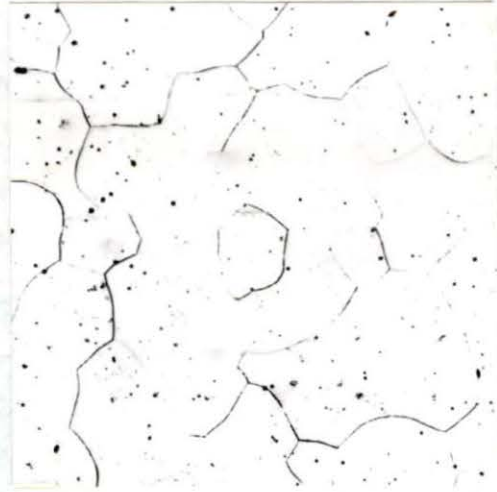
Fig. 24.
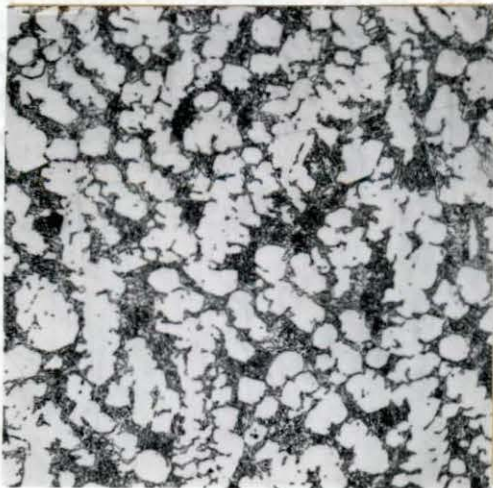
Fig. 25.
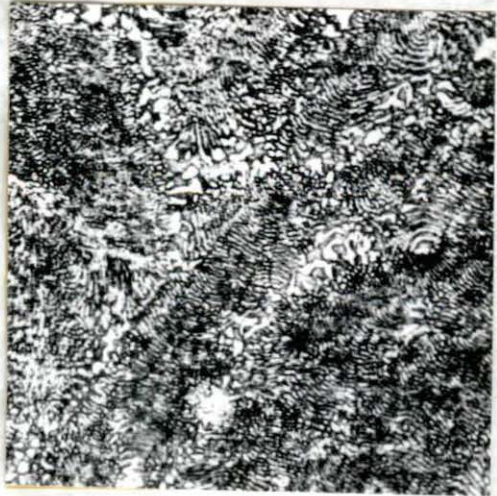
Fig. 26.

Fig. 27. 0.33 at. % Y. Annealed at 1250°C for
1 hour and cooled rapidly. Ni plus
Y_2Ni_{17} (eutectic). Etched 5 seconds
in Carapella's reagent. X100.

Fig. 28. 0.14 at. % Y. Annealed at 1250°C for
1 hour and cooled rapidly. Ni plus
slight amount of Y_2Ni_{17} (eutectic).
Etched 5 seconds in Carapella's re-
agent. X100.

Table 2. X-ray diffraction results.

Compound	Crystal class	Space group	Lattice parameters (in Å)	Molecules per unit cell	Density	
					X-ray (g./cc.)	Measured (g./cc.)
Y_3Ni	?					
Y_3Ni_2	?					
YNi	ortho-rhombic	?	a = 4.10±.02 b = 5.51±.02 c = 7.12±.02	4	6.10	6.00
YNi_2	f.c.c.	O_h^7-Fd3m (C_{15} type)	a_0 = 7.181±.001	8	7.40	7.33
YNi_3	rhombo-hedral	(allowable) R$\bar{3}$m R3m R32	a = 8.60±.02 α = 33°48'	3	7.55	7.53
Y_2Ni_7	?					
YNi_4	?					

Table 2 (continued).

Compound	Crystal class	Space group	Lattice parameters (in Å)	Molecules per unit cell	Density	
					X-ray (g./cc.)	Measured (g./cc.)
YNi_5	hexag-onal	D_{6h}^1-	$a_o=4.883\pm.001$	1	7.75	7.84
		C6/mmm	$c_o=3.967\pm.001$			
Y_2Ni_{17}	hexag-onal	(allowable) C6/mmc C6mc C$\bar{6}$2c	$a = 8.34\pm.02$ $c = 8.08\pm.02$	2	8.01	8.23

1. Y_3Ni

Due to the complexity of the powder pattern of this compound, difficulty was encountered in picking a unique unit cell.

2. Y_3Ni_2

X-ray powder patterns of this compound also were very complex.

3. YNi

Single crystals of this compound were obtained from shrinkage cavities in a 53.0 at. % Ni alloy. It was found to be orthorhombic with mmm Laue symmetry and the following lattice constants: a = 4.10Å, b = 5.51Å, and c = 7.12Å. On the basis of 4 molecules per unit cell a density of 6.10 g./cc. was calculated, which is in good agreement with the measured value of 6.00 g./cc.

4. YNi_2

Powder patterns of an alloy containing 66.7 at. % Ni annealed at 950°C for 100 hours showed YNi_2 to be f.c.c. with $a_0 = 7.181 \pm .001$Å. YNi_2 appeared to be isostructural with the parameterless $MgCu_2$ structure, and this was confirmed by comparing calculated and observed intensities for YNi_2. The structure has the space group O_h^7 - Fd3m with

8 Y at: 000; 1/4,1/4,1/4; + f.c.

16 Ni at: 5/8,5/8,5/8; 7/8,7/8,5/8; 7/8,5/8,7/8;
5/8,7/8,7/8; + f.c.

This structure is the C_{15} type - Laves phase. Table 3 gives the observed and calculated $\sin^2 \theta$ and intensity values for YNi_2. The distances of closest approach obtained from the above lattice constant are: Y - Y = 3.109 Å, Ni - Ni = 2.538 Å, and Ni - Y = 2.977 Å.

A composition range was proposed for this compound from metallographic evidence. To confirm this composition range, X-ray powder patterns were taken of 65.2 and 68.1 at. % Ni alloys which had been annealed at $950^{\circ}C$ for 100 hours and quenched. Lattice constants and unit cell volumes obtained were a_o = 7.183 ± .002Å ----- V = 370.47Å^3 and a_o = 7.164 ± .001Å ----- V = 367.58Å^3 or a contraction of 2.89Å^3 from the yttrium rich to the nickel rich side. A substitution of 1 atom of nickel (8.08Å^3) for 1 atom of yttrium (25.53Å^3) per 6 unit cells would account for this contraction. If this is the case the composition range would be approximately 0.7 at. %. Since the 65.2 and 66.7 at. % Ni alloys had the same lattice constants, it was assumed the composition range extended to the nickel rich side of YNi_2 as shown in Fig. 2.

The lattice constants of analogous compounds of lanthanum, cerium and praseodymium with nickel are listed in Table 4.

Table 3. Observed and calculated $\sin^2\theta$ and intensity values for YNi_2.

Index	$\sin^2\theta_{obs.}$	$\sin^2\theta_{calc.}$	$I_{obs.}$	$I_{calc.}$
111	-----	.03457	-----	.4
200	-----	.04610	-----	0
220	.09385	.09220	VSt	6,216
311	.12843	.12677	VVSt	15,310
222	.14033	.13830	VSt	4,269
400	.18684	.18440	VVW	144
331	.21925	.21897	-----	2.6
420	-----	.23050	-----	0
422	.27893	.27659	M	2,245
511, 333	.31319	.31117	VSt	4,400
440	.37042	.36879	St	3,489
531	-----	.40337	-----	28
600	-----	.41489	-----	0
620	.45833	.46099	VVW	93
533	.49406	.49557	M	1,652
622	.50559	.50709	M	1,493
444	-----	.55319	-----	28
711, 551	-----	.58776	-----	74
640	-----	.59929	-----	0
642	.64602	.64539	W	1,438
731, 553	.67984	.67996	St	2,760
800	.73704	.73759	VW	1,049
733	-----	.77216	-----	71
820, 644	-----	.78369	-----	0
822, 660	.82895	.82978	VW	1,383
751, 555	.86305 (α_1)	.86291	St	2,737
	.86781 (α_2)	.86727	W	
662	.87425 (α_1)	.87441	M	1,829
	.87884 (α_2)	.87883	VW	

Table 4. Lattice constants of some Laves phases.

Compound	Lattice constant in $\overset{o}{A}$
$LaNi_2$	7.24^a
$PrNi_2$	7.191^a
$CeNi_2$	7.189^b
	7.178^c

[a]The value of $LaNi_2$ is somewhat uncertain. See Vogel (4).

[b]See Fulling et al. (12).

[c]See Nowotny (13).

The composition range of YNi_2 noted in the present study could explain the discrepancy in the lattice constants of $CeNi_2$ reported by Fulling et al. (12) and by Nowotny (13), since no attempt was made by these authors to establish a composition range for $CeNi_2$. The uncertainty in the value for $LaNi_2$ could also have resulted from a change in lattice constants with composition.

There is a contraction of $0.49\overset{o}{A}$ in Y - Y distance in YNi_2 as compared to yttrium metal. The contraction of the Ce - Ce ($0.53\overset{o}{A}$), La - La ($0.58\overset{o}{A}$) and Pr - Pr ($0.53\overset{o}{A}$) distances in the RNi_2 phase is explained by Laves (14) primarily on the basis of strong polar forces, since electron

transfer from lanthanum to nickel will not account for this large contraction. However, Pauling (15) does explain the La - La contraction in $LaNi_2$ on the basis of electron transfer from nickel to lanthanum.

5. YNi_2

Single crystal studies on this compound showed it to have $\bar{3}m$ Laue symmetry. Observed reflections were $-h + k + l = 3n$, $h\bar{h}l$ where $l = 3n$, and hhl where $h + l = 3n$; therefore, the possible space groups are $R\bar{3}m$, $R3m$ and $R32$. The non-primitive hexagonal unit cell dimensions determined from rotation patterns are $a = 5.00\overset{o}{A}$ and $c = 24.30\overset{o}{A}$. Referred to the primitive rhombohedral cell they become: $a = 8.60\overset{o}{A}$ and $\alpha = 33°48'$. The density calculated on the basis of 9 molecules per hexagonal cell was 7.55 g./cc. while the density measured pycnometrically was 7.53 g./cc. confirming the stoichiometry YNi_3.

6. Y_2Ni_7

Powder patterns of this compound were quite complex and attempts to index the patterns were unsuccessful.

7. YNi_4

The lines on powder patterns of this compound were diffuse and attempts to index the patterns were unsuccessful.

8. $\underline{YNi_5}$

Powder patterns of an alloy containing 83.4 at. % Ni showed YNi_5 to be hexagonal with $a_o = 4.883 \pm .001\overset{o}{A}$ and $c_o = 3.967 \pm .001\overset{o}{A}$. YNi_5 appeared to be isostructural with the parameterless $CaCu_5$ structure, and this was confirmed by comparing calculated and observed intensities of YNi_5. This structure has the space group $D_{6h}^1 - C6/mmm$ with

1 Y at: $(0,0,0)$

2 Ni at: $\pm (1/3,2/3,0)$

3 Ni at: $(0,1/2,1/2)$; $(1/2,0,1/2)$; $(1/2,1/2,1/2)$

The calculated and observed $\sin^2\theta$ and intensity values for YNi_5 are given in Table 5 and the interatomic distances are given in Table 6. (The observed $\sin^2\theta$ and intensity values were those of an 83.4 at. % Ni alloy.)

The variation in lattice constants with composition in this compound appeared to be mostly in the "a" direction. The lattice constants of YNi_5 obtained from an 82.0 at. % Ni alloy which had been annealed at $1150^\circ C$ and quenched are $a_o = 4.890 \pm .005\overset{o}{A}$ and $c_o = 3.962 \pm .005\overset{o}{A}$; while those obtained from an 84.5 at. % Ni alloy annealed at $1150^\circ C$ and quenched were $a_o = 4.865 \pm .005\overset{o}{A}$ and $c_o = 3.967 \pm .005\overset{o}{A}$.

9. $\underline{Y_2Ni_{17}}$

Single crystals of this compound were obtained from shrinkage cavities in a 91.5 at. % Ni alloy. It is

Table 5. Observed and calculated $\sin^2\theta$ and intensity values for YNi_5.

Index	$\sin^2\theta_{obs.}$	$\sin^2\theta_{calc.}$	$I_{obs.}$	$I_{calc.}$
100	-----	.03323	-----	133
001	-----	.03776	-----	23
101	.07241	.07099	St	591
110	.10079	.09970	St	534
200	.13444	.13210	St	674
111	.13924	.13746	VVSt	2069
002	.15280	.15106	St	653
201	.17210	.16986	St	500
102	-----	.18429	-----	18
210	-----	.23180	-----	12
112	.25181	.25076	M	230
211	.27332	.26956	W	143
202	.28585	.28316	M-St	366
300	.30095	.29909	W	86
301	.33755	.33685	St	437
003	-----	.33988	-----	.8
103	.37431	.37311	VVW	41
212	-----	.38286	-----	10
220	.39894	.39879	M-St	348
310	-----	.43202	-----	4
221	-----	.43655	-----	3
113	.44113	.43958	M-St	296
302	.45243	.45015	W	87
311)	.47157	.46978	W	(58
203)		.47198		(84
400	.53366	.53172	W	71
222	.55105	.54985	VSt	476
401)	.57357	.56948	W	(70
213)		.57168		(49
312	-----	.58308	-----	6
004	.60618	.60416	VW	77
320	-----	.63142	-----	3
104	-----	.63739	-----	3
303	.64083	.63897	M	215
321	.67069	.66918	VVW	47
402	.68374	.68278	M	128
410	.69825	.69788	VW	67
114	.70623	.70386	VW	67
411)		.73564		(446
204)	.73674	.73626	VSt	(134
223)		.73867		(3
313	.77276	.77190	VW	54

Table 5 (continued).

Index	$\sin^2\theta_{obs.}$	$\sin^2\theta_{calc.}$	$I_{obs.}$	$I_{calc.}$
322	-----	.78248	-----	5
500	-----	.83081	-----	1.5
214	-----	.83596	-----	6
412	.84950	.84894	M	174
501	-----	.86857	-----	34
403	.87028	.87160	W	92
330	-----	.89728	-----	52
304	.90286 (α_1)	.90179	W	108
	.90645 (α_2)	.90634		
420	.92984 (α_1)	.92895	M	248
	.93336 (α_2)	.93363		
331	.93336 (α_1)	.93347	St	423
	.93765 (α_2)	.93818		
005	-----	.94725	-----	1
323	.96949 (α_1)	.96966	M	141
	.97466 (α_2)	.97426		

Table 6. Interatomic distances in YNi_5.

Reference atom	Neighboring atoms	Distance (in Å)
Y	6Ni	2.821
	12Ni	3.147
Ni_1	3Y	2.821
	6Ni	2.433
Ni_2	4Y	3.147
	4Ni	2.442
	4Ni	2.433

hexagonal with 6/mmm Laue symmetry and the following lattice constants: $a = 8.34\overset{\circ}{A}$ and $c = 8.08\overset{\circ}{A}$. The only systematic extinctions were hhl for odd l so the allowed space groups are C6/mmc, C6mc and $C\bar{6}2c$. The same Laue symmetry and systematic extinctions were found by Florio et al. (16) in Th_2Ni_{17}. By spatial and symmetry arguments, they concluded Th_2Ni_{17} belongs to the space group C6/mmc. Since the r (12) radius of yttrium is $1.797\overset{\circ}{A}$ and thorium is $1.795\overset{\circ}{A}$ (17), Y_2Ni_{17} probably also belongs to the C6/mmc space group.

D. Magnetic Transition Temperature Results

The magnetic transition temperature of primary nickel was unaltered by the addition of yttrium. None of the intermetallic compounds in this system were magnetic at room temperature.

E. Yttrium Allotropy

The existence of an α-β transformation and the temperature at which the transformation occurs have been primarily established by indirect experimental evidence as discussed below. Since the transformation occurs so close to the melting point of yttrium, direct experimental evidence for the transformation is difficult even in the pure metal. In the present study, difficulty due to the presence of a

liquid phase in alloys containing more than 0.1 at. % Ni was
also encountered. Electrical resistivity studies on alloys
containing 0.04 and 0.08 at. % Ni were unfruitful due to the
small resistivity change which accompanies the $\alpha-\beta$ transfor-
mation. Since the solubility of nickel in α yttrium is very
low, it is unlikely that the $\alpha-\beta$ transformation was altered
appreciably by the addition of nickel.

Evidence for the transformation of yttrium to a b.c.c.
phase was obtained from alloy studies of yttrium with other
metals that have a high temperature b.c.c. form, and with
magnesium. In the yttrium-lanthanum system, Valletta (18)
found a continuous series of solid solutions at high temper-
ature, thus indicating the hexagonal to b.c.c. transforma-
tion of yttrium. He estimated the transformation tempera-
ture to be 1460 to 1490°C from extrapolated thermal data of
the beginning and end of a transformation from hexagonal
yttrium solid solution region to a high temperature b.c.c.
solid solution region. Eash and Carlson (19) obtained a
temperature of 1490°C for the $\alpha-\beta$ transformation of yttrium
from similar extrapolation of thermal data in the Th-Y sys-
tem and electrical resistivity measurements on pure yttrium.

Gibson and Carlson (20) in a study of the Y-Mg system
were able to quench a 1 phase magnesium-90% Y alloy from
900°C. The 1 phase was b.c.c. with an approximate lattice

constant of 3.90Å. The same alloy on slow cooling exhibited an eutectoid structure.

IV. DISCUSSION

The general features of the nickel-yttrium phase system of low terminal solubility and a large number of compounds were expected from a consideration of Hume-Rothery's rules and phase diagrams of the rare earths with elements of the first transition series, respectively. Since yttrium appeared to be forming more compounds than cerium with elements of the first transition series, a greater number of compounds was expected in the nickel-yttrium system than in the cerium-nickel system; this, too, was found to be the case.

In discussing the alloying behavior of yttrium with the transition elements listed in Table 7, two observations are pertinent. The first is that no compounds are formed with titanium, vanadium and chromium, while compound formation occurs with manganese, iron, cobalt and nickel and the second is that an increasing number of compounds is formed between yttrium and manganese, iron, cobalt and nickel. This alloying behavior is rather surprising when one considers the great similarity between each of the elements of the first transition series listed in Table 7 in size, electronegativity and valence.

To explain the first observation, the theory proposed by Pauling (21) fits quite well. He used the terms hypoelectronic, hyperelectronic and buffer atoms and defined

Table 7. Pertinent data on some of the d-transition elements.

Element	Radius (r12)[a]	Electro-negativity[b]	Pauling's[a] valence	Number of compounds formed with yttrium
Y	1.797	1.2	3	--
Ti	1.467	1.6	4	0
V	1.338	1.7	5	0
Cr	1.276	1.6	6	0
Mn	1.268	1.5	6	>1
Fe	1.260	1.7	6	4 or 5
Co	1.252	1.7	6	?
Ni	1.244	1.8	6	9

[a]See Pauling (15).

[b]See Gordy (22).

them as follows: "Hypoelectronic atoms are atoms that can increase their valence by adding electrons; Hyperelectronic atoms are atoms that can increase their valence by giving up an electron; Buffer atoms are atoms that can give up or accept an electron without change in valence." He divides the elements into these 3 categories as shown in Table 8. He then proposes that the strongest tendency toward

Table 8. Classification of atoms with respect to effect of change of electron number on metallic valence.

Hypoelectronic atoms					Atoms with stable valence					Hyperelectronic atoms						
Li	Be	B					C					N	O	F		
Na	Mg	Al					Si					P	S	Cl		

<div align="center">Buffer atoms</div>

K	Ca	Sc	Ti	V	Cr[a]	Mn	Fe	Cr	Ni	Cu	Zn	Ga	Ge	As	Se	Br
Rb	Sr	Y	Zr	Nb	Mo[a]	Tc	Ru	Rh	Pd	Ag	Cd	In	Sn	Sb	Te	I
Cs	Ba	La	Ce[b]													
	Lu	Hf	Ta		W[a]	Re	Os	Ir	Pt	Au	Hg	Tl	Pb	Bi	Po	At

[a]These 3 atoms can accept electrons but not give up electrons without change in valence.

[b]The rare-earth metals may have some buffering power.

compound formation is between elements of different groups. Therefore, we would not expect compound formation between yttrium and titanium, vanadium or chromium. (Chromium is hypoelectronic with respect to yttrium since it can only accept electrons without changing its valence.) Also, we would expect compound formation between yttrium and manganese, iron, cobalt and nickel.

Although any attempted explanation for the increase in the number of intermetallic compounds formed between yttrium and manganese, iron, cobalt and nickel is mostly conjecture without a complete structure analysis of all the compounds present in these systems, it appears that the progressively greater number of 3d electrons present must be the determining factor. Within a particular alloy system, such as nickel-yttrium, it might be possible with a complete structure analysis of each compound to show the primary stabilizing factor for each compound to be geometric; but when one considers the small difference in the atomic radii of iron and nickel, it is difficult to imagine size alone to be the reason for the iron-yttrium system having 5 fewer compounds than the nickel-yttrium system. The small electronegativity difference between iron and nickel also does not appear to explain the difference in the number of compounds present in the iron-yttrium and nickel-yttrium systems. Pauling's metallic valences listed in Table 7 show equal valence for

iron and nickel; however, according to Massalski (23) the valency of a transition metal may vary in different alloy systems and also vary with composition in a single system. If we then assume a greater variableness in valency as the number of 3d electrons increases, an increase in the number of compounds would be expected in going from manganese to nickel due to the increase in the number of bonds possible.

Another possible approach to the problem would be to consider the various types of compounds formed in these systems. Most structure types which have been studied extensively have been explained generally on the basis of electron to atom ratios. Hume-Rothery's "electron compounds" is the classical example of structure types stabilized by a definite electron to atom ratio. Duwez (24) summarizes attempts by various authors to rationalize the sigma phase in systems of the transition metals on the basis of electron to atom ratio. Raynor (25) proposes that the stabilizing factor for some compounds of aluminum with the transition elements is a constant electron to atom ratio. On the other hand, structure types such as Laves phases appear to be stabilized primarily by size effects with polar forces (14) having an effect in some cases.

If we assume that a half filled 3d shell is a stable configuration, that is, the electrons in a half filled shell do not take part in compound formation, then compounds

formed in the yttrium-manganese system should be those sta-
bilized primarily by size effects. Since the atomic radii
of iron, cobalt and nickel are essentially the same as man-
ganese, the compounds stabilized by size should also appear
in the iron, cobalt and nickel systems with yttrium. Any
additional compounds formed in the iron-yttrium system
should then be compounds stabilized by an electron to atom
ratio. Since in cobalt, two 3d electrons over the stable
half filled shell are available, a greater number of com-
pounds stabilized by an electron to atom ratio should be
present and a still greater number in the nickel-yttrium
system.

Some credence may be given the above discussion by the
fact that the Laves type phase (AB_2) is present in the man-
ganese (3), iron (3), and nickel and possibly cobalt systems
with yttrium. As stated before, a complete structure analy-
sis of all the compounds present in these systems would be
most informative.

V. SUMMARY

The nickel-yttrium phase system has been established from results of thermal, metallographic and X-ray studies. General features which were found are low melting eutectics, a large number of compounds, and low terminal solubility.

There are eutectics at 34.8, 57.5, and 93.3 at. % Ni which melt at $805^{\circ}C$, $950^{\circ}C$ and $1285^{\circ}C$ respectively. There are 9 intermetallic compounds, with YNi and YNi_5 melting congruently at $1070^{\circ}C$ and $1430^{\circ}C$ respectively, while the remaining compounds, Y_3Ni, Y_3Ni_2, YNi_2, YNi_3, Y_2Ni_7, YNi_4 and Y_2Ni_{17}, decompose peritectically at $902^{\circ}C$, $820^{\circ}C$, $1106^{\circ}C$, $1237^{\circ}C$, $1298^{\circ}C$, $1340^{\circ}C$, and $1330^{\circ}C$ respectively.

The following crystallographic data for YNi, YNi_3, and Y_2Ni_{17} were obtained by single crystal methods: YNi is orthorhombic with a = 4.10Å, b = 5.51Å, and c = 7.12Å; YNi_3 is rhombohedral with a = 8.60Å and α = $33^{\circ}48'$; Y_2Ni_{17} is hexagonal with a = 8.34Å and c = 8.08Å. The compounds YNi_2 and YNi_5 appeared to be isostructural with the parameterless structures $MgCu_2$ and $CaCu_5$ respectively which was confirmed in both cases by comparing calculated and observed intensities. YNi_2 is f.c.c. with a_o = 7.181±.001Å and belongs to the O_h^7—Fd3m space group while YNi_5 is hexagonal with a_o=4.883±.001Å and c_o=3.967±.001Å and belongs to the D_{6h}^1—C6/mmm space group. The formulas of Y_3Ni, Y_3Ni2, Y_2Ni_7

and YNi_4 were proposed from metallographic evidence and their presence was confirmed by X-ray diffraction studies.

The magnetic transition temperature of primary nickel was unaltered by the addition of yttrium. None of the intermetallic compounds were magnetic at room temperature.

The solubility of nickel in yttrium was found to be approximately 0.2 at. % at $900^\circ C$ and the solubility of yttrium in nickel was found to be approximately 0.1 at. % at $1250^\circ C$.

VI. LITERATURE CITED

1. Haefling, J.F. and Daane, A. H., Trans. Met. Soc. A.I.M.E., 215, 336 (1959).

2. Fisher, R. and Fullhart, C., Feasibility studies on molten metal reactor components. United States Atomic Energy Commission Report ISC-1020 [Iowa State College] (1956).

3. Haefling, J. F., Yttrium alloy studies. (Research Notebook No. 8), Ames, Iowa, Iowa State College, Ames Laboratory of the Atomic Energy Commission (1957).

4. Vogel, R., Z. Metallkunde, 38, 97 (1947).

5. Bare, D. W., The yttrium-titanium phase diagram. (Research Notebook No. 1), Ames, Iowa, Iowa State College, Ames Laboratory of the Atomic Energy Commission (1957).

6. Jepson, J. O. and Duwez, P., Trans. Am. Soc. Metals, 47, 543 (1955).

7. Wensch, G. W. and Whyte, D. D., The nickel-plutonium system. United States Atomic Energy Commission Report LA-1304 [Los Alamos Scientific Laboratory of the University of California] (1951).

8. Konobeevsky, S. T., Equilibrium diagrams of certain systems based on plutonium. Proceedings of the Conference on the Peaceful Uses of Atomic Energy, Moscow, Chemical Science, 211 (1955).

9. Ellinger, F. H., Review of the intermetallic compounds of plutonium. Conference on the Metal Plutonium, Sponsored by The U. S. Atomic Energy Commission and The American Society for Metals, Chicago, Illinois (1957) [to be published by The American Society for Metals, ca, 1959].

10. Pirani, M. and Alterthum, H., Z. Elektrochem., 29, 5 (1923).

11. Cohen, M. U., Rev. Sci. Instruments, 6, 68 (1935); 7, 155 (1936).

12. Fulling, W., Moeller, K. and Vogel, R., Z. Metallkunde, 34, 253 (1942).

13. Nowotny, H., Z. Metallkunde, 34, 247 (1942).

14. Laves, F., Crystal structure and atomic size. In American Society for Metals, ed. Theory of alloy phases. pp. 124-198. Cleveland, Ohio (1956).

15. Pauling, L., The electronic structure of metals and alloys. In American Society for Metals, ed. Theory of alloy phases. pp. 220-242. Cleveland, Ohio (1956).

16. Florio, J.V., Baenziger, N. C. and Rundle, R. E., Acta Cryst., 9, 367 (1956).

17. Pauling, L., J. Am. Chem. Soc., 69, 542 (1947).

18. Valletta, R. M., The yttrium-lanthanum phase system. (Research Notebook No. 1), Ames, Iowa, Iowa State College, Ames Laboratory of the Atomic Energy Commission (1959).

19. Eash, D. T. and Carlson, O. N., Investigation of the thorium-yttrium system and the allotropy of yttrium. United States Atomic Energy Commission Report ISC-1146 [Iowa State College] (1959).

20. Gibson, E. D. and Carlson, O. N., The yttrium-magnesium system. United States Atomic Energy Commission Report ISC-1152 [Iowa State College] (1959).

21. Pauling, L., Proc. Nat. Acad. Sci. U.S., 36, 533 (1950).

22. Gordy, W., Physical Review, 69, No. 604 (1946).

23. Massalski, T. B., Intermediate phases and electronic
     structure. In American Society for Metals, ed. Theory
     of alloy phases. pp. 63-123. Cleveland, Ohio (1956).

24. Duwez, P., Intermediate phases in alloys of the tran-
     sition elements. In American Society for Metals, ed.
     Theory of alloy phases. pp. 243-254. Cleveland, Ohio
     (1956).

25. Raynor, G. V., Progress in the theory of alloys. In
     Chalmers, B., ed. Progress in metal physics. Vol. 1,
     pp. 1-76. London, Butterworth Scientific Publications
     (1949).

VII. ACKNOWLEDGMENTS